Electronic spectrum of S_2^-, the electron affinity of S_2, and the binding energies of neutral and anionic S_3 clusters

Christoph Heinemann and Wolfram Koch*
Institut für Organische Chemie der Technischen Universität Berlin, Straße des 17 Juni 135, D-10623 Berlin, Germany

Gottlieb-Georg Lindner and Dirk Reinen
Fachbereich Chemie, Philipps-Universität Marburg, Hans-Meerwein-Strasse, D-35032 Marburg, Germany
(Received 29 November 1994)

The low-lying electronic states of the S_2^- anion have been investigated by quantum-chemical methods incorporating an extensive treatment of electron correlation. All excited doublet states that can be reached in spin- and dipole-allowed transitions from the $^2\Pi_g$ ground state of the anionic disulfur molecule as well as the lowest quartet state $^4\Sigma_u^-$ are characterized by their spectroscopic constants, excitation energies, and transition dipole matrix elements with the ground state. Furthermore, an accurate calibration of the employed theoretical methods with respect to the electron affinity of the sulfur atom, the potential energy curves for the ground states of S_2 and S_2^-, the electron affinity of S_2, and the binding energies of the neutral and anionic S_3 clusters is presented.

PACS number(s): 33.20.−t, 31.25.Nj, 32.10.Hq, 33.15.Fm

I. INTRODUCTION

Homonuclear negatively charged diatomic and triatomic molecules from the sixth main group of the Periodic Table of elements have attracted growing interest over the past years from both the experimental and the theoretical point of view. Many of the available spectroscopic data have been obtained from ultraviolet and visible spectroscopy [1], Raman [2], luminescence [3], and electron spin resonance [4] experiments of the O_2^-, O_3^-, S_2^-, S_3^-, Se_2^-, and Te_2^- species isolated in alkali halide or silicate host matrices. In addition to these matrix experiments, the gaseous O_2^-, O_3^-, S_2^-, S_3^-, and Se_2^- molecules have been studied by means of photoelectron (PE) and photodetachment spectroscopy [5] and the chemical reactivity of various anionic sulfur clusters in the gas phase has been investigated by different mass-spectrometric techniques [6]. In the assignment and interpretation of some of the spectroscopic data quantum-chemical calculations have proved to be useful. As examples we mention studies on the low-lying electronic states of O_2^- [7], O_3^- [8], and S_3^- [9], which gave information on potential-energy surfaces, transition energies, and spectral intensities. An additional challenge connected with these investigations was the accurate calculation of electron affinities [10], which still remains one of the open problems for highly accurate calculations on atoms, diatomic, and small polyatomic molecules [11].

The principal subject of the present theoretical investigation is the disulfur anion S_2^-, which has recently been investigated experimentally under various conditions: The S_2^- molecule has been prepared in the gas phase from reactions of ions with molecules [6] and its electron affinity was measured as 1.670±0.015 eV by PE spectroscopy [5(e),12]. Furthermore, the equilibrium internuclear distance for S_2^- was determined as 3.790±0.028 bohrs and the frequency of its ground state could be deduced from a vibrational progression as 570±100 cm^{-1}. The vibrational frequency in the electronic ground state of S_2^- was also measured as 584 cm^{-1} [Raman experiments in sodalith [2(b)] and 614 cm^{-1} [luminescence experiments in potassium bromide [3(c)]] in solid matrices and the 0-0 line of an electronic transition to an electronically excited state was found to occur between 19 100 and 19 600 cm^{-1} for S_2^--doped alkali iodides (NaI, KI, and RbI) [3(c)]. In the corresponding bromides and chlorides a shift to higher energies is observed, presumably due to compressive crystal field effects from the matrix [3(c)].

In general, theoretical data on the diatomic anions of oxygen, sulfur, and selenium, in particular with respect to electronically excited states, are scarce. Thus experimentalists usually interpreted results on the S_2^- and Se_2^- systems, in particular the transition energies from the ground state to electronically excited states, on the basis of the only *ab initio* study available for the full electronic spectrum of O_2^-, an early multiconfiguration self-consistent field study by Krauss *et al.*, in which all 24 molecular states correlating with the energetically most favorable $O(^3P)+O^-(^2P)$ asymptote were investigated [7(a)]. Unfortunately, this very detailed study cannot provide quantitatively reliable data for transition energies since the level of the calculation, in both the treatment of the n-particle space and the employed one-particle basis sets, was relatively low, as compared to modern standards. Regarding the quite different energetic separations of the low-lying terms of the oxygen and sulfur atoms [13], it may even appear questionable whether the oxygen calculations can qualitatively, with respect to the relative ordering of the electronic states, be transferred to the cases of the higher chalcogenides. On the other hand,

*Author to whom correspondence should be addressed.

molecular-orbital arguments strongly suggest that the ground states of S_2^- and Se_2^- are also of $^2\Pi_g$ symmetry, deriving from the $^3\Sigma_g^-$ ground states of the neutral diatomic molecules by introducing an additional electron in an antibonding π_g $3p$ orbital (see Fig. 1).

Two theoretical studies of S_2^- have been performed earlier: Cotton, Harmon, and Hedges employed the density-functional $X\alpha$ method to calculate the excitation energy between the $^2\Pi_g$ and $^2\Pi_u$ states of this anion [14] and Ramondo, Sanna, and Bencivenni used Møller-Plesset perturbation theory to investigate the structure and binding energy of the ion pair Li^+ S_2^- [15]. Furthermore, the S_2^- molecule is part of the G2 set of molecules [16], which provides a standard reference for the accuracy of quantum-chemical methods.

The purpose of the present study is to provide accurate *ab initio* information on those parts of the electronic spectrum of the disulfur anion that are most relevant for the optical absorption and luminescence experiments. High-quality wave functions, incorporating an extensive treatment of electron correlation, are presented for the $^2\Pi_g$ ground state of S_2^- and those excited states correlating with the atomic ground states $S(^3P)+S^-(^2P)$, which are accessible in spin-allowed electric-dipole transitions from the S_2^- ground state. There are six states of this kind, two of both the $^2\Pi_u$ and $^2\Sigma_u^-$ types plus one $^2\Sigma_u^+$ and one $^2\Delta_u$ term. From the respective potential-energy curves, spectroscopic constants for all states are calculated and the corresponding transition dipole elements will be given. In addition, we have considered the lowest-lying quartet state $^4\Sigma_u^-$. An estimate of the probability of a transition between this state and parts of the doublet manifold can be based on an evaluation of the corresponding spin-orbit matrix elements. Finally, the present study investigates the performance of the high-quality *ab initio* wave functions for the description of the electron affinity of the sulfur atom and the disulfur molecule as well as the binding energies of S_3 and S_3^- with respect to S_2 and $S(S^-)$. A calibration of the available highly correlated methods will be appreciated in future theoretical work on Se_x^- and Te_x^- ($x=2,3$) [17], which represent already large problems for accurate quantum-chemical investigations.

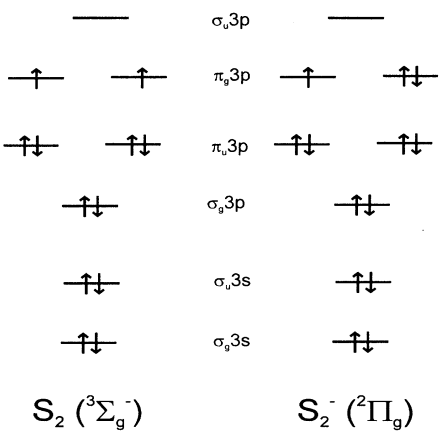

FIG. 1. Molecular-orbital diagrams for the ground states of S_2 and S_2^-.

II. THEORETICAL METHODS

Most of the wave functions presented in this study are of the multireference configuration interaction (MRCI) type [18]. The linear expansion of the wave function Ψ is partitioned in a reference space comprising a small number (up to 15) of configuration state functions (CSFs) necessary for a proper description of the dissociation of a molecular state in a given symmetry and the much larger $[(1-2)\times 10^6]$ space of external CSFs generated by all symmetry-adapted single and double excitations from each reference function into the virtual orbitals:

$$\Psi_{\mathrm{MRCI}}=\sum_l \left\{ C(I)\phi(I)+\sum_{i,a} C_i^a(I)\phi_i^a(I) + \sum_{i,j,a,b} C_{ij}^{ab}(I)\phi_{ij}^{ab}(I) \right\} .$$

Here the index l runs over all reference states and ij and ab denote the occupied and virtual orbitals to a given reference configuration. In this treatment, different correlation effects are taken care of in a balanced manner. The particular choice of the reference space ensures the proper behavior of the wave function in the asymptotic dissociation limit and the description of near-degeneracy effects ("nondynamic" correlation), while through the excitations in the external space additional "dynamic" spatial and radial correlation deriving from the r_{ij}^{-1} term in the Hamiltonian is incorporated in the wave function. However, this CI approach has the disadvantage of missing size consistency [19].

In the first step, complete active space self-consistent field (CAS-SCF) calculations [20] were carried out in order to generate the orbitals for the subsequent MRCI calculations and to identify the reference configurations: All symmetry-adapted CSFs for the 13 (12 for S_2) active valence electrons of S_2^- ($3s$ and $3p$ orbitals of the separated atoms) were generated (the 10 core orbitals with the $1s$, $2s$, and $2p$ electrons were kept doubly occupied [21]) and the CAS-SCF wave function Ψ_{CAS} was obtained by variationally minimizing the energy expectation value $\langle \Psi_{\mathrm{CAS}}|H|\Psi_{\mathrm{CAS}}\rangle$ with respect to the expansion coefficients and orbitals. For the given state the resulting wave functions were investigated at several internuclear distances near the equilibrium geometry and in the dissociation limit and a particular CAS-SCF configuration was selected for the MRCI reference space if the coefficient of at least one spin coupling in the CAS-SCF expansion exceeded the threshold value of 0.05 at any internuclear distance. The second step consisted of the calculation of the adiabatic potential-energy curves from separate MRCI calculations at 15–25 internuclear distances. For each state the MRCI expansion was carried out in the natural orbitals of the respective CAS-SCF wave function. Single and double excitations from all spin couplings generated by the reference configurations were part of the MRCI expansion throughout which the 20 core electrons were kept uncorrelated (i.e., these electrons were not excited

into the virtual space [21]). The reference states, the number of spin couplings in the reference space, and the total length of the different MRCI expansions are summarized in Table I.

The MRCI equations were solved iteratively by the direct method as implemented in the MOLCAS-2 suite of programs [22]. Usually 8–10 iterations (15–20 for the higher excited states) were necessary to achieve the final MRCI energy E_{MRCI} (convergence threshold $\Delta E_{\mathrm{MRCI}} \leq 10^{-7}$ hartree), which is a true upper bound to the exact nonrelativistic energy. Since the present singles plus doubles methodology is not size extensive, the multireference analog of the renormalized Davidson correction [23] was applied to achieve approximate size consistency for the final energies $E_{\mathrm{MRCI+Q}}$:

$$E_{\mathrm{MRCI+Q}} = E_{\mathrm{MRCI}} + \Delta E_c \frac{1-c_0^2}{c_0^2} .$$

Here ΔE_c denotes the energy difference between the MRCI energy and the energy of the reference wave function and c_0^2 is the weight of the reference space in the total MRCI expansion.

In the third step, the MRCI+Q energies served to generate analytic expressions for the potential-energy curves by fitting cubic polynomials to the computed energies. In the resulting potential, the rovibrational spectrum for each state was calculated by a numeric solution of the Schrödinger equation for the nuclei according to Numerov's method using a grid of 299 points for the numerical integration at internuclear distances from 3–10 bohrs. To investigate the optical absorption of S_2^- ions, transition dipole moments between the ground state and all states accessible under the electric-dipole approximation were calculated at the MRCI+Q equilibrium distance of the electronic ground state ($R_e = 3.815$) from CAS-SCF wave functions. To avoid systematic errors due to the nonorthogonality of natural CAS orbitals belonging to different states of the same symmetry, the CAS state interaction method was employed [24].

Although the most important part of this study was carried out in the multireference "philosophy," at certain points comparisons to coupled-cluster theory [25] were made, which should give a hint of the importance of higher than double excitations in the treatment of dynamical correlation. The coupled-cluster including all single and double excitations (CCSD) wave function is of the form

$$\Psi_{\mathrm{CCSD}} = e^{T_1+T_2}\Psi_{\mathrm{HF}} ,$$

where Ψ_{HF} denotes a Hartree-Fock [restricted open-shell Hartree-Fock (ROHF) in the general case] reference configuration while T_1 and T_2 are the respective single and double excitation operators. Their effect is to generate all symmetry-adapted single and double excitations from the Hartree-Fock reference. Due to the higher powers of T_1 and T_2, the Ψ_{CCSD} wave function includes not only single and double excitations, but also higher excitations of all orders, where the coefficients of these high-order excitations are given exclusively as products of the single and double excitations. The presence of such disconnected clusters, which are absent in a configuration interaction including all single and double excitations from a single Hartree-Fock reference (CISD) wave function, is why a CCSD usually is superior to a CISD [25].

An additional noniterative and perturbative treatment of the triple excitations is denoted CCSD(T). As "many-body" techniques both CCSD and CCSD(T) have the advantage of being size-extensive methods; however, they are *nonvariational* in the sense that neither E_{CCSD} nor $E_{\mathrm{CCSD(T)}}$ represents an upper bound to the true ground-state energy of a given system.

Two aspects of the effects of spin-orbit coupling on the electronic structure of S_2^- were evaluated: First, the fine-structure splittings (FSSs) of the lowest $^2\Pi$ states of S_2^- in their $^2\Pi_{1/2}$ and $^2\Pi_{3/2}$ components were evaluated at the CAS-SCF level using a well-established approach

TABLE I. Multireference CI expansions for the ground states of S_2 and S_2^- and excited states of S_2^-. The table contains the occupation numbers of the partially occupied orbitals in the selected reference configurations for the MRCI wave function, the resulting number of spin couplings, and the total length of the MRCI expansion. The orbitals are given in the order $4a_g 5a_g 2b_{3u} 2b_{2u} 4b_{1u} 5b_{1u} 2b_{2g} 2b_{3g}$.

	S_2	S_2^-							
State	$^3\Sigma_g^-$	$^2\Pi_g$	$^2\Delta_u$	$^2\Pi_u$(I)	$^2\Sigma_u^+$	$^2\Sigma_u^-$(I)	$^2\Pi_u$(II)	$^2\Sigma_u^-$(II)	$^4\Sigma_u^-$
Reference configurations	22 222 011	22 222 012	22 222 111	22 212 220	22 222 120	22 212 220	22 212 220	22 222 111	21 122 221
	21 212 112	21 122 122	22 112 122	22 212 022	22 222 102	22 212 022	22 212 022	21 212 212	21 212 212
	21 122 121	20 222 212	21 212 212	21 222 121	22 220 122	21 222 121	22 211 122	21 122 221	22 112 122
	20 222 211		21 122 221	20 212 222	22 202 122	20 212 222	21 222 121	22 112 122	22 222 111
	22 112 022				22 022 122	12 122 221	22 122 211		
	20 112 222				20 222 122	12 212 212			
Number of spin couplings	10	4	8	5	10	12	8	8	4
Total number of CSFs in MRCI	1 349 652	560 500	1 175 385	678 703	1 312 393	1 523 135	1 111 809	1 175 385	1 050 272

based on the one-electron part of the Breit-Pauli Hamiltonian [26]

$$H_{\text{s.o.}} = (\alpha^2/2) \sum_{i,a} Z(a) r_{ia}^{-3} (\mathbf{r}_{ia} \times \mathbf{p}_i) \cdot \mathbf{s}_i \ .$$

Here α denotes the fine-structure constant, $\mathbf{r}_{ia}$ is the distance of the ith electron from the ath nucleus, $\mathbf{p}_i$ is the momentum of electron i, $\mathbf{s}_i$ is its spin, and $Z(a)$ is the nuclear charge of atom a. The FSS is then computed as twice the matrix element $\langle {}^2\Pi_g | H_{\text{s.o.}} | {}^2\Pi_g \rangle$, where, due to the use of the D_{2h} point group (see Sec. III B), the irreducible representations of the bra and the ket wave functions were chosen as ${}^2B_{2g}$ and ${}^2B_{3g}$, respectively. An easy semiempirical way to account for the computationally much more demanding two-electron terms is to adjust $Z(a)$ to an effective value by fitting calculated FSSs to known experimental values. In a recent application Koseki, Schmidt, and Gordon determined Z_{eff} for sulfur in the 6-31G^* basis as 13.8 from a parametrization on the FSSs of SH, SH^+, and SH^- [27]. However, this value gave a conceivable underestimation of the FSS of S_2^- with respect to the experimental value, which led us to maintain $Z_{\text{eff}}(S)$ as 16 for the present purposes, thus restricting the spin-orbit calculations to the more important one-electron part. In addition to the fine-structure splittings, spin-orbit coupling matrix elements $\langle {}^4\Sigma_u^- | H_{\text{s.o.}} | {}^2\Psi \rangle$ between the lowest quartet state ${}^4\Sigma_u^-$ and all bound doublet states ${}^2\Psi$ were evaluated. In all cases the ten inactive core orbitals were those determined for the ${}^4\Sigma_u^-$ state of S_2^- and the valence orbitals were individually optimized for the ${}^4\Sigma_u^-$ and the respective doublet state at the CAS-SCF level of theory. The spin-orbit matrix elements were then calculated in C_1 symmetry (program limitations) using the optimized orbitals for each state and converging the CI iterations to the desired state, such that both CI coefficients and the total energy were identical to the calculation in full symmetry.

All orbitals were expanded in a generally contracted Gaussian basis set of the atomic natural orbital (ANO) type [28], which has been designed to give an accurate description of atomic ionization potentials, electron affinities, and polarizabilities and should thus be well suited for the present purpose. The $17s12p5d4f$ primitive set was contracted to $6s5p4d3f$ according to Widmark, Perrson, and Roos [28(b)]. As test calculations (see below) indicated the need for higher-angular-momentum basis functions, a single g exponent α_g was optimized for the description of the atomic electron affinity of sulfur ($\alpha_g = 0.732$) and an even scaling procedure (with the ratio between two exponents being 2.5) served to generate two g-type basis functions that augmented the original ANO basis to the final $6s5p4d3f2g$ form with 80 contractions per sulfur atom (spherical harmonic polarization functions, i.e., $5d$, $7f$, and $9g$ components were employed). For the spin-orbit calculations the $(12s9p)/[6s5p]$ McLean-Chandler basis set [29] was employed. Two d-type polarization functions (with exponents 1.300 and 0.325, six Cartesian components each) were added to obtain a final set of triple-ζ plus two polarization functions quality.

All calculations with the MOLCAS-2 suite of programs were carried out on IBM RS/6000 workstations. Using the full 12MWord memory of a model 370 machine the average computational effort per single-point calculation (i.e., generation and transformation of the integrals, CAS-SCF calculation, and solution of the MRCI equations) amounts to approximately 3.5 h of CPU time and 6 h of real time, respectively. Coupled-cluster calculations employed the open-shell CCSD and CCSD(T) codes from ACES-2 [30] and MOLPRO94 [31] and were performed on our IBM workstations and the CRAY-YMP computers of the Konrad-Zuse Zentrum, Berlin. The program system GAMESS [32], as installed on IBM RS/6000 workstations, was used for the spin-orbit calculations.

III. RESULTS AND DISCUSSION

A. Calibration of the employed methods

To investigate the reliability of the employed methods test calculations on the electron affinity and the low-lying excited states of the sulfur atom were carried out. Three ANO contractions, here denoted ANO1 ($6s5p3d2f$ contraction), ANO2 (enlargement of the $spdf$ part by one contraction $7s6p4d3f$), and ANO3 ($6s5p4d3f2g$, the basis finally selected for the study of S_2 and its anion), served to investigate basis set convergence. The results, collected in Table II, allow an evaluation of the basis set quality and the performance of different correlation treatments for the present purposes.

The experimental electron affinity (EA) of the sulfur atom amounts to 2.08 eV [33]. At the CAS-SCF level, which is equivalent to a single-configuration ROHF wave function for S and S^-, a value of 0.90 eV is calculated with all three ANO contractions. As expected, dynamic correlation is much more important for the S^- anion than for the neutral atom and thus the configuration-interaction treatment (denoted CISD since in this case single and double excitations from a single ROHF reference were generated) improves the result considerably with an ANO3 value of 1.80 eV. Starting with the ANO1 basis (with an EA of 1.73 eV), it is more important to incorporate the g-type functions in the one-particle space than to increase the number of s, p, d, or f contractions (see Table II: the EA with the ANO2 basis is identical to the ANO1 level). Higher than double excitations account for most of the remaining error as compared to the experimental value, as can clearly be seen from the effects of the Davidson correction (an approximate way to treat "unlinked" quadruple excitations [23]), which increases all calculated electron affinities by more than 0.1 eV with a final CISD+Q–ANO3 value of 1.95 eV. CISD results for the electron affinity of the sulfur atom, calculated with augmented correlation-consistent (AUG-CC) basis sets, have recently been reported by Woon and Dunning [34]. Their most accurate CISD value, calculated with the augmented correlation-consistent polarized valence quadrupole zeta (HUG-CC-pVQZ) basis ($7s6p4d3f2g$ contraction of a $17s12p4d3f2g$ primitive set), amounts to 1.78 eV, very close to the ANO3 result presented here. Note, however, that the convergence properties of the correlation-consistent basis with respect to the electron

affinity of the sulfur atom were different from those for the ANOs employed here: The addition of diffuse s and p functions, which are already included in the primitive ANO set [35], has the most important influence on the electron affinity of sulfur when the AUG-CC-pVQZ basis is generated. Furthermore, Woon and Dunning have indicated the need for extended CAS-SCF and MRCI wave functions if one wants to calculate the electron affinity of the sulfur atom with high accuracy. In contrast to this conclusion, we find that a multireference strategy is not mandatory for this goal: Moreover, an increased treatment of dynamic correlation starting from a simple Hartree-Fock reference function improves the theoretical EAs considerably, as is evident from the CCSD-ANO3 and CCSD(T)-ANO3 results of 1.94 and 2.03 eV. The latter result is already close to "chemical accuracy" of 1 kcal/mol (=0.04 eV). Finally, the introduction of higher-angular-momentum functions eventually leads to a convergence of the theoretical EAs towards the experimental value: First a single h function with an exponent of 0.6, which was optimized with respect to the EA of sulfur, was added to ANO3, which increased the CCSD(T) electron affinity to 2.049 eV (the CCSD result was 1.959 eV). Since the $spdf$ part of ANO3 was already rather saturated for this purpose (see above), in a second step only the number of higher-angular-momentum polarization functions was increased to three g-type and two h-type functions by an even-scaling procedure, which gave theoretical EAs of 1.968 eV (CCSD) and 2.059 eV [CCSD(T)]. Further enlargement of the fg part of the basis set (four g-type and three h-type even-scaled functions) did not improve the calculated EAs considerably [CCSD, 1.969 eV; CCSD(T), 2.061 eV]. Therefore, a single i function with an exponent of 0.5 was added to the $6s5p4d3f3g2h$ basis resulting in a $6s5p4d3f3g2h1i$ contraction in which the CCSD(T) electron affinity amounts to 2.064 eV (CCSD, 1.973 eV). Generation of two even-scaled i functions around the exponent of 0.5 slightly raises this result to 1.975 eV (CCSD) and 2.066 eV [CCSD(T)]. This basis set consists of 181 primitives and 137 contractions and is too large for molecular applications even those involving only two sulfur atoms. On the other hand, it is now possible to estimate the errors in the present calculation of the sulfur electron affinity: The final difference between the theoretical and the experimental electron affinity amounts to merely 0.011 eV.

This error reflects the sum of the contributions from the following remaining error sources in the calculated electron affinity of the sulfur atom: Insufficient treatment of the n-particle space, core-core and core-valence correlation effects (which cannot be adequately treated using the standard ANO basis sets of this study [21]), and relativistic contributions. The completeness of the CCSD(T) method for the treatment of the n-particle space was checked by a comparison between a valence full configuration-interaction [36] (VFCI) calculation in which all possible sixfold and sevenfold excitations for S (six valence electrons) and S^- (seven valence electrons) are included in the CI expansion with a CCSD(T) calculation using the $5s4p2d1f$ ANO contraction in both bases.

TABLE II. Theoretical and experimental energies for the ground and low-lying excited states of the sulfur atom and its anion.

		ANO1		ANO2		ANO3	
Species	Method	E_{tot} (hartree)	E_{rel} (eV)	E_{tot} (hartree)	E_{rel} (eV)	E_{tot} (hartree)	E_{rel} (eV)
$S(^3P)$	CAS	−397.506 06	0.00	−397.506 11	0.00	−397.506 07	0.00
	CISD	−397.652 01	0.00	−397.653 22	0.00	−397.658 13	0.00
	CISD+Q	−397.662 88	0.00	−397.664 15	0.00	−397.669 40	0.00
	CCSD	−397.655 86	0.00	−397.657 10	0.00	−397.660 64	0.00
	CCSD(T)	−397.661 35	0.00	−397.662 73	0.00	−397.666 69	0.00
	Expt.[a]						0.00
$S(^1D)$	CAS	−397.455 87	1.37	−397.455 94	1.37	−397.455 90	1.37
	CISD	−397.608 53	1.18	−397.609 89	1.18	−397.615 68	1.16
	CISD+Q	−397.620 63	1.15	−397.622 06	1.15	−397.628 30	1.12
	Expt.[a]						1.12
$S(^1S)$	CAS	−397.373 51	3.61	−397.373 55	3.61	−397.373 51	3.61
	CISD	−397.549 66	2.79	−397.551 06	2.78	−397.557 30	2.74
	CISD+Q	−397.560 12	2.80	−397.561 57	2.79	−397.568 27	2.75
	Expt.[a]						2.75
$S^-(^2P)$	CAS	−397.539 27	−0.90	−397.539 32	−0.90	−397.539 29	−0.90
	CISD	−397.715 50	−1.73	−397.716 92	−1.73	−397.724 33	−1.80
	CISD+Q	−397.731 58	−1.87	−397.733 11	−1.88	−397.741 18	−1.95
	CCSD	−397.724 24	−1.86	−397.725 72	−1.87	−397.731 95	−1.94
	CCSD(T)	−397.732 80	−1.94	−397.734 50	−1.95	−397.741 26	−2.03
	Expt.[b]						−2.08

[a]Reference [13].
[b]Reference [33].

This is the largest basis set in which a VFCI calculation can still be carried out within our hardware limits. Also in these VFCI calculations the ten core electrons are not correlated. The resulting electron affinities amount to 1.906 eV (VFCI) and 1.901 eV [CCSD(T)]. The same basis set gives electron affinities of 1.696 and 1.837 eV on the CISD and the CISD+Q levels of theory [37]. These results reveal that, at least within a basis set of approximately triple-ζ quality augmented by two d-type and one f-type polarization [TZ(2Pf)] functions [38], the treatment of the n-particle space by the CCSD(T) method is very close to the VFCI limit, in contrast to a truncated CI expansion (CISD). Unfortunately, the high computational cost of the VFCI method does not allow for a similar comparison using the "best" ANO-derived $6s5p4d3f3g2h1i$ basis and the convergence properties of the CCSD(T) and FCI electron affinities with the size of the basis set are not necessarily identical. However, based on the TZ(2Pf) comparison we estimate an error of 0.010 ± 0.005 eV from the insufficient treatment of the n-particle space in the computed electron affinity of the sulfur atom. As far as relativistic effects are concerned, we find that the addition of the Darwin and mass-velocity operators to the Hamiltonian and computing the perturbational first-order relativistic correction to the total energies *decreases* the computed atomic sulfur electron affinity to a small extent (at the MCRI+Q–ANO3 level the computed EA drops by 0.008 eV) [39]. The order of magnitude for spin-orbit effects, which are not included in our one-component treatment, can be estimated from the experimentally known fine-structure splitting of the ^3P term of the sulfur atom S and the corresponding value for $S^-(^2P)$. While the experimental energy for the process $S(^3P_2)+e^-\rightarrow S^-(^2P_{3/2})$ amounts to 2.077 eV, a value of 2.081 eV results if both atomic terms are taken as weighted averages over all spin-orbit levels, which is the correct experimental reference to the computed EAs. Thus, together with the scalar relativistic corrections and the estimated contribution from insufficient treatment of the n-particle space, one arrives at a final deviation of 0.013 ± 0.005 eV (105 ± 40 cm^{-1}) between the theoretical and the experimental electron affinities. This is the order of magnitude for core-core correlation and the core-valence correlation contributions to the electron affinity of the sulfur atom. Among these, the latter should be more relevant since the additional electron of the anion resides in the valence $3p$ orbital, which has a local maximum in the L shell of the core region [40].

As far as electronic excitation energies for the sulfur atom are concerned, we have investigated the ^3P, ^1D, and ^1S terms arising from the ground state $3p^4$ configuration. The experimental excitation energies from the ground state ^3P term, taken as a weighted average over its three spin-orbit components, to the excited ^1D and ^1S states amount to 1.12 and 2.75 eV, respectively. Both processes are excellently described by the MRCI wave functions presented in this study: Employing the largest basis set, ANO3, the MRCI+Q excitation energies (see Table II) exactly match the experimental results, with only very small contributions (0.01 eV) from the Davidson correction. Furthermore, the smaller ANO1 and ANO2 contractions give only slightly different results. On the other hand, the CAS-SCF method overestimates the relative energy of the excited state energy for both cases (see Table III).

B. Molecular symmetry

Since the SEWARD integral generator in the employed MOLCAS-2 program system is restricted to the use of Abelian point groups, D_{2h} rather than the true $D_{\infty h}$ symmetry was imposed throughout the whole study. Thus the degenerate $^2\Pi_g$, $^2\Pi_u$, and $^2\Delta_u$ states are resolved into $^2B_{2g}$-$^2B_{3g}$, $^2B_{2u}$-$^3B_{3u}$, and $^2B_{1u}$-^2A_u components, respectively. Identifications of the Π states is straightforward within the electronic spectrum. However, the $^2\Delta_u$ state correlates with ^2A_u and $^2B_{1u}$ as do the $^2\Sigma_u^-(^2A_u)$ and $^2\Sigma_u^+(^2B_{1u})$ states, which makes it necessary to individually optimize the two lowest MRCI roots in the $^2B_{1u}$ and the lowest three MRCI roots in the ^2A_u irreducible representations in order to identify the terms unambiguously. It turns out that for internuclear distances greater than 4 bohrs the first root in $^2B_{1u}$ symmetry is numerically identical to the first ^2A_u root within the expected deviations (average value of 2 mhartree $=0.05$ eV), which are due to the somewhat different lengths of the respective MRCI expansions (see Table I). The corresponding wave function was thus identified as the $^2\Delta_u$ state. For internuclear distances less than 4 bohrs this state is still the lowest MRCI root in $^2B_{1u}$ symmetry, while it becomes the second ^2A_u root. The first ^2A_u root in this range and, in turn, the second ^2A_u root for internuclear distances greater than 4 bohrs is thus identified as the first $^2\Sigma_u^-$ state, later denoted $^2\Sigma_u^-$(I), and the third ^2A_u root is the second $^2\Sigma_u^-$ state, $^2\Sigma_u^-$(II). With these assignments, the second $^2B_{1u}$ root over the whole internuclear range is recognized as the $^2\Sigma_u^+$ state. The low-lying quartet state was calculated in ^4A_u symmetry and could, in $D_{\infty h}$, thus either be of $^4\Delta_u$ or $^4\Sigma_u^-$ symmetry. In accord with the earlier results on O_2^- [7] it is evident that the $^4\Sigma_u^-$ state corresponds to this first ^4A_u root, which can also be inferred from qualitative molecular-orbital considerations (see Fig. 1): Promotion of an electron from the antibonding π_g $3p$ to the antibonding σ_u $3p$ orbital, resulting in a $^4\Sigma_u^-$ wave function, should be the energetically most favorable way to generate a quartet state from the $^2\Pi_g$ ground state of S_2^-.

Finally, we comment on the errors introduced for the dissociation limits by maintaining a center of inversion along the internuclear separation coordinate. In a study of the low-lying states of N_2^{2+} Taylor has pointed out [41] that CAS-SCF energies in asymmetric dissociation limits (in which the atomic states differ in charge and/or in the atomic terms) of a homonuclear diatomic molecule tend to be too high compared to the separate atoms. Since the CAS-SCF is a size-consistent method, the effect must be attributed to the deficiencies of a finite basis set: Namely, if the two atomic states exhibit very different electronic distributions, the employed one-particle set is not flexible enough to represent the "molecular" orbitals as accurately as in separate atomic situations because the

TABLE III. Multireference CI wave functions for the ground states of S_2 and S_2^- and excited states of S_2^-. The table contains all CSFs of the MRCI expansion with coefficients $c > 0.05$, their respective spin couplings (3, doubly occupied; 1, high-spin coupled singly occupied; 2, low-spin coupled singly occupied; 0, empty) for the valence molecular orbitals, and the total weight of the reference space in the MRCI wave function.

State	$4a_g$	$5a_g$	$2b_{3u}$	$2b_{2u}$	$4b_{1u}$	$5b_{1u}$	$2b_{2g}$	$2b_{3g}$	Coefficient	Reference weight (%)
S_2										
$^3\Sigma_g^-$(R =3.60 bohrs)	3	0	3	3	3	3	1	1	−0.066	88.2
	3	1	1	3	3	2	3	1	0.068	
	3	1	2	3	3	1	3	1	−0.052	
	3	1	3	1	3	3	1	3	−0.069	
	3	1	3	2	3	1	1	3	0.052	
	3	3	1	1	3	0	3	3	−0.116	
	3	3	3	3	3	0	1	1	0.921	
S_2^-										
$^2\Pi_g$(R =3.80 bohrs)	3	0	3	3	3	3	1	3	−0.081	8.74
	3	1	1	3	3	2	3	3	0.092	
	3	1	2	3	3	1	3	3	−0.070	
	3	3	3	3	3	0	1	3	0.924	
$^2\Delta_u$(R =4.70 bohrs)	3	1	1	3	3	3	3	2	0.054	86.7
	3	1	2	3	3	3	3	1	0.078	
	3	1	3	1	3	3	2	3	0.054	
	3	3	1	2	3	1	3	3	0.367	
	3	3	3	3	3	1	1	2	0.732	
	3	3	3	3	3	1	2	1	0.422	
$^2\Pi_u$(R =4.50 bohrs)	3	0	3	1	3	3	3	3	0.108	86.8
	3	1	3	3	3	1	3	2	0.104	
	3	1	3	3	3	2	3	1	−0.265	
	3	3	3	1	3	0	3	3	0.879	
	3	3	3	1	3	3	3	0	−0.058	
$^2\Sigma_u^+$(R =4.90 bohrs)	3	1	2	3	3	3	1	3	0.078	86.8
	3	1	3	2	3	3	3	1	0.078	
	3	3	0	3	3	1	3	3	0.325	
	3	3	3	0	3	1	3	3	0.325	
	3	3	3	3	3	1	0	3	0.566	
	3	3	3	3	3	1	3	0	0.566	
$^2\Sigma_u^-$(I)(R =4.40 bohrs)	3	1	2	3	3	3	3	1	−0.114	86.2
	3	1	3	2	3	3	1	3	0.114	
	3	3	1	1	3	2	3	3	−0.205	
	3	3	3	3	3	1	1	2	−0.446	
	3	3	3	3	3	1	2	1	0.770	
$^2\Pi_u$(II)(R =4.50 bohrs)	3	1	3	3	3	1	3	2	0.917	86.3
	3	1	3	3	3	2	3	1	0.066	
	3	3	3	1	1	2	3	3	0.026	
	3	3	3	1	2	1	3	3	−0.068	
	3	3	3	1	3	0	3	3	−0.087	
	3	3	3	1	3	3	3	0	0.054	
$^2\Sigma_u^-$(II)(R =4.50 bohrs)	3	1	1	3	3	3	3	2	0.210	85.2
	3	1	2	3	3	3	3	1	−0.200	
	3	1	3	1	3	3	2	3	−0.210	
	3	1	3	2	3	3	1	3	0.200	
	3	3	1	1	3	2	3	3	0.819	
	3	3	3	3	3	1	1	2	−0.058	
	3	3	3	3	3	1	2	1	0.099	
$^4\Sigma_u^-$(R =4.50 bohrs)	3	1	1	3	3	3	3	1	0.101	86.7
	3	1	3	1	3	3	1	3	−0.101	
	3	3	1	1	3	1	3	3	−0.245	
	3	3	3	3	3	1	1	1	0.887	

center of inversion forces them to be delocalized along the molecular axis even in the asymptotic dissociation limit. We stress that the missing size consistency of the CAS-SCF method in such a case is not a violation of basic quantum-mechanical principles, but rather a technical problem, which, as Taylor has already pointed out, can be overcome by including additional CSFs in the wave function. For the ground state of S_2^- the situation is the following: At the CAS-SCF level, the sum of the separated atom energies $S(^3P)+S^-(^2P)$ amounts to $-795.045\,36$ hartree. The dissociation limit ($R=50$ bohrs) in D_{2h} symmetry, however, has a CAS-SCF energy of $-795.017\,96$ hartree, 27 mhartree higher than the separated atoms. Reducing the symmetry in the dissociation limit to C_{2v} allows for the localization of the additional electron on one sulfur atom and the CAS-SCF energy ($-795.045\,37$) is identical to the separated atoms. At $R=5$ bohrs, however, both the C_{2v} and the D_{2h} calculations give the same CAS-SCF energy, indicating that it is only at the dissociation limit that the (already fairly large) finite basis set of the present study is not flexible enough to describe molecular orbitals in the composite system, which matches exactly the electronic situation found for the separate components. On the other hand, the MRCI treatment is able to counterbalance this deficiency at the CAS-SCF level: The MRCI and MRCI+Q energies in D_{2h} and C_{2v} symmetry at $R=50$ bohrs differ only by 1.4 and 0.6 mhartree, respectively. We conclude that at this level, maintaining a center of inversion along the whole internuclear range does not affect the computed properties.

It is also instructive to compare the molecular dissociation limit of S_2^- with the separate atoms at the MRCI and MRCI+Q levels: The separated atoms are lower than the molecular dissociation limit by 32.6 and 8.2 mhartree, respectively. Although the Davidson correction recovers 75% of the deviation due to size inconsistency, the remaining difference is still in the range of 5 kcal/mol, far from chemical accuracy (1 kcal/mol). We conclude that already for the a system as small as S_2^- with only the 13 valence electrons, size consistency must be regarded as a major issue if binding energies of small molecules or clusters are calculated from separated fragments.

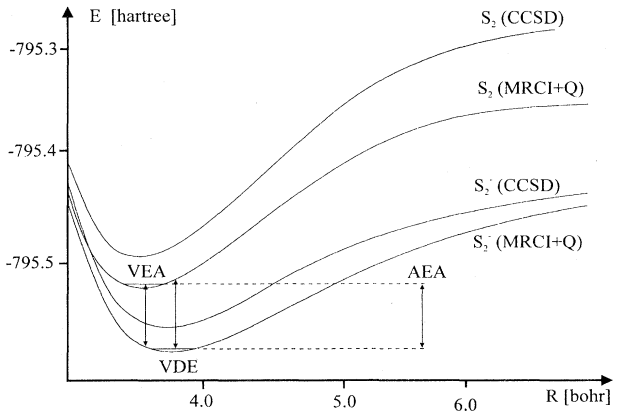

FIG. 2. CCSD and MRCI+Q potential-energy curves for the ground states of S_2 and S_2^-. The adiabatic electron affinity (AEA), the vertical electron affinity (VEA), and the vertical detachment energy (VDE) have been indicated for the MRCI+Q potentials.

C. Ground states of S_2 and S_2^-

The MRCI+Q–ANO3 and CCSD-ANO3 potential-energy curves for the $^3\Sigma_g^-$ and $^2\Pi_g$ ground states of S_2 and S_2^- are displayed in Fig. 2. Corresponding MRCI+Q–ANO3 total energies and spectroscopic constants are listed in Tables IV and V. An inspection of the MRCI wave functions (Table III) shows that both species are well described by the chosen reference spaces, for which the weights in the total MRCI expansion amounts to nearly 90%. As is evident from the number of important ($|c|>0.05$) configurations and the weights of the leading configurations near the equilibrium distances, the neutral S_2 species (with one empty orbital and two half-filled orbitals in the leading CSF) is of higher multiconfigurational character than its anionic counterpart, which has only one empty orbital and one half-filled orbital in the Hartree-Fock configuration.

In general, fair agreement between experimental (as far as available) and theoretical properties is found for these two molecules. The theoretical equilibrium bond distance of 3.605 bohrs for S_2 is somewhat longer than the experimental value (3.571 bohrs [42]) and the calculated

TABLE IV. Selected total MRCI+Q energies for the ground states of S_2 and S_2^- and excited states of S_2^- (in hartree).

	S_2	S_2^-							
R (bohrs)	$^3\Sigma_g^-$	$^2\Pi_g$	$^2\Delta_u$	$^2\Pi_u$(I)	$^2\Sigma_u^+$	$^2\Sigma_u^-$(I)	$^2\Pi_u$(II)	$^2\Sigma_u^-$(II)	$^4\Sigma_u^-$
3.00	−795.393 51	−795.402 59	−795.292 67	−795.183 37	−795.273 25	−795.310 59	−795.101 68	−794.989 32	−795.318 31
3.50	−795.491 67	−795.534 47	−795.409 93	−795.386 33	−795.392 29	−795.420 60	−795.245 58	−795.124 16	−795.436 56
3.80	−795.488 42	−795.547 92	−795.429 72	−795.433 32	−795.414 57	−795.435 07	−795.275 66	−795.197 19	−795.456 21
4.00	−795.476 14	−795.545 09	−795.437 86	−795.448 91	−795.424 56	−795.439 54	−795.305 26	−795.237 84	−795.463 60
4.20	−795.460 12	−795.537 29	−795.443 36	−795.456 86	−795.431 72	−795.442 07	−795.325 46	−795.272 62	−795.468 24
4.40	−795.442 57	−795.526 77	−795.446 78	−795.459 77	−795.436 72	−795.443 04	−795.341 72	−795.301 15	−795.470 42
4.60	−795.424 88	−795.515 02	−795.448 33	−795.459 37	−795.439 0	−795.442 75	−795.354 23	−795.323 94	−795.470 54
4.80	−795.408 01	−795.503 02	−795.448 38	−795.456 90	−795.441 26	−795.441 25	−795.363 55	−795.341 84	−795.469 10
5.00	−795.392 63	−795.491 35	−795.447 31	−795.453 19	−795.441 47	−795.438 79	−795.370 27	−795.355 76	−795.466 58
50.00	−795.333 72	−795.402 37	−795.404 11	−795.402 66	−795.404 09	−795.404 97	−794.402 21	−795.403 59	−795.404 28

TABLE V. Spectroscopic constants for the ground states of S_2 and S_2^- and excited states of S_2^- based on MRCI+Q potential-energy curves.

	S_2	S_2^-					
Property	$^3\Sigma_g^-$[a]	$^2\Pi_g$[b]	$^2\Delta_u$	$^2\Pi_u$(I)	$^2\Sigma_u^+$	$^2\Sigma_u^-$(I)	$^4\Sigma_u^-$
R_e (bohrs)	3.605[c]	3.815[d]	4.720	4.469	4.940	4.444	4.512
D_e (eV)	4.35	3.96	1.21	1.56	1.02	1.10	1.81
D_o (eV)	4.30[e]	3.92[f]	1.19	1.54	1.00	1.08	1.79
ω_e (cm^{-1})	734[g]	582[h]	236	340	205	224	270
B_e (cm^{-1})	0.300	0.267	0.170	0.192	0.154	0.191	0.185

[a]Results from the CCSD potential-energy curve: $R_e=3.580$ bohrs, $D_e=3.95$ eV, $D_0=3.90$ eV, $\omega_e=807$ cm^{-1}, and $B_e=0.292$ cm^{-1}. D_e at the CCSD(T) level: 4.30 eV.
[b]Results from the CCSD potential-energy curve: $R_e=3.794$ bohrs, $D_e=3.66$ eV, $D_0=3.62$ eV, $\omega_e=635$ cm^{-1}, and $B_e=0.257$ cm^{-1}. D_e at the CCSD(T) level: 3.93 eV.
[c]Experimental value: 3.571 bohrs [42].
[d]Experimental value: (3.790±0.028) bohrs [5(e)].
[e]Experimental value: 4.41 eV [42].
[f]Experimental value: 4.05 eV [5(e)].
[g]Experimental value: 726 cm^{-1} [42].
[h]Experimental value: 570±100 cm^{-1} [5(e)].

vibrational frequency (734 cm^{-1}) matches the experimental one (726 cm^{-1} [42]) with a deviation of 1%. An earlier MRCI+Q study of O_2, which in terms of technical details is quite similar to the present investigation on S_2, overestimated the experimental bond length by only 0.011 bohrs [43]. Most probably, core-valence correlation effects are the main error source responsible for the unexpectedly large deviation between the calculated (MRCI+Q) and the experimental bond length in neutral S_2: If the 2*s* and 2*p* electrons are included in the correlation treatment, the sulfur-sulfur distance is reduced to 3.593 bohrs. However, in this case the bond dissociation energy (see below) is *overestimated* by 0.4 eV, which we attribute to the fact that the ANO3 basis does not incorporate steep functions of higher angular momentum, which are required for a proper description for core-valence correlation [21]. The detailed investigation of core-valence correlation effects in diatomic second-row molecules remains a task for future theoretical studies. Since the extra electron of the anion occupies an antibonding orbital, the MRCI+Q bond length for S_2^- (3.815 bohrs) is longer compared to the neutral molecule (an earlier MP2/6-31+G* calculation gave a very similar result of 3.832 bohrs for the bond length of the S_2^- ground state [15]). For comparison, the experimentally deduced bond length is 3.790±0.028 bohrs [5(e)] and we conclude from the comparison of theoretical and experimental data for the neutral S_2 molecule that the true value will most probably lie close to the center of the bond length interval derived by photoelectron spectroscopy. The theoretical vibrational frequency for the ground state of S_2^- (582 cm^{-1}) is within the large experimental error limit for the free S_2^- species (570±100 cm^{-1}) and compares well to the value of 584 cm^{-1}, derived from Raman spectroscopy of S_2^- in silicate host matrices [2(b)]. Again following the results for the neutral S_2 ground state, for which our theoretical frequency is 8 cm^{-1} higher than the experimental value, we conclude that the true vibrational frequency of S_2^- is around 570 cm^{-1}.

Finally, the MRCI+Q bond dissociation energies for both S_2 (4.30 eV) and S_2^- (3.92 eV) match the experimental results [S_2, 4.41 eV [42]; S_2^-, 4.05 eV [5(e)]] to within 0.15 eV, which is a satisfactory result but still 250% from "chemical accuracy." The respective MRCI values amount to 4.10 and 4.00 eV, respectively. The effect of the Davidson correction is relatively small for the bond energy of S_2^-, but amounts to more than 0.22 eV (=5 kcal/mol) for the neutral counterpart. However, all other spectroscopic constants for both molecules are only marginally affected by the Davidson correction (MRCI data for S_2, $R_e=3.601$ bohrs and $\omega_e=725$ cm^{-1}; for S_2^-, $R_e=3.813$ bohrs and $\omega_e=568$ cm^{-1}).

For comparison, we have also calculated the potential-energy curves for the ground states of S_2 and S_2^- using the ROHF-based CCSD method. The results are shown in Fig. 2 as well and spectroscopic constants have been included in Table V. We summarize the performance of CCSD as follows. (i) The S—S bond is calculated to be shorter, i.e., closer to the experimental values, by 0.02 bohrs as compared to the MRCI in both cases (for S_2, 3.580 bohrs; S_2^-, 3.794 bohr; CCSD deviations from the experimental results are less than 0.01 bohrs). (ii) The CCSD frequency for S_2 (807 cm^{-1}) exceeds the MRCI+Q and experimental values by 10%. The reason for this overestimation is evident from Fig. 2, which shows that the corresponding potential energy curve is still reminiscent of the Hartree-Fock reference function, which is known to lead to a too high dissociation limit [44]. S_2^-, which has less multiconfigurational character, is much better described at the CCSD level ($\omega_e=635$ cm^{-1}, compared to 582 cm^{-1} for MRCI+Q). (iii) The CCSD bond dissociation energies are lower by 0.40 eV (S_2) and 0.30 eV (S_2^-) than the corresponding MRCI+Q values. The somehow larger deviation for S_2 as compared to S_2^- can again be attributed to the fact that at the equi-

librium internuclear distance the S_2 molecule has a somewhat higher multiconfigurational character as compared to S_2^-. CCSD(T), which includes a perturbative inclusion of the triple excitations, improves the CCSD bond energies for S_2 and S_2^- considerably to final values of 4.30 and 3.97 eV. It should be mentioned that the basis set superposition error (BSSE) in the present calculations is rather small: When using the ANO3 contraction, the counterpoise correction [45], which should give an upper limit to the BSSE [46], amounts to 0.6 kcal/mol for the bond energy of S_2.

D. Electron affinity of S_2

The experimental electron affinity of S_2 has been determined in a photodetachment experiment as 1.670 ± 0.015 eV [5(e)]. This value corresponds to the adiabatic 0-0 transition between the ground states of S_2 and S_2^- and will be referred to as the adiabatic electron affinity. The contribution of the zero-point vibrational energy to the electron affinity of S_2 amounts to -0.01 eV (see Sec. III C) and will not be explicitly included in the following discussion, because it is an order of magnitude smaller than the expected overall error of the calculations. As expected from the calibration studies and former experience [8,9,11], the theoretically determined adiabatic electron affinities of S_2 (see Table VI) are below the experimental result: The MRCI+Q results with the ANO3 basis amounts to 1.48 eV, with an important contribution of 0.19 from the size-consistency correction. With the ANO2 contraction, which does not include g-type basis functions, the computed MRCI+Q electron affinity is smaller by 0.06 eV, indicating that, similar to the S atom, the employed basis sets are not yet saturated for the higher-angular-momentum components. The CAS-SCF treatment, which mainly includes nondynamic correlation effects, yields a value of 0.66 eV for the adiabatic electron affinity of S_2. The single-reference Hartree-Fock method gives, however, a higher value (0.99 eV), because it shows a bias towards the S_2^- species, for which a single configuration is a better approximation as compared to S_2 (see the discussion above). Consequently, the surprisingly good performance of the SCF-based CCSD (1.65 eV) and CCSD(T) (1.65 eV) methods partly benefits from a fortuitous cancellation of errors. In Fig. 2, this can be recognized by the different upward shifts of the CCSD with respect to the MRCI+Q potential-energy curves. Although one might have expected that the more extensive treatment of electron correlation in the CCSD(T) method *increases* the computed electron affinity of S_2, the inclusion of the perturbative triples does not change the CCSD value of 1.65 eV, which obviously indicates that parts of the CCSD deficiencies due to its single reference function are compensated at the CCSD(T) level. On the other hand, the calibration studies on the sulfur atom (see Sec. III A) have shown the superiority of the coupled-cluster approach to the configuration-interaction approach for the treatment of dynamic correlation in single-reference cases. Therefore, we expect that multireference coupled-cluster theory, which is presently an area of active development [47], seems a good candidate for a powerful and predictive tool for the computation of electron affinities when different degrees of multiconfigurational character are present for a neutral and its anion. Finally, the computed electron affinities can be compared to earlier studies: Fourth-order Møller-Plesset perturbation theory in a basis set of triple-ζ quality (MP4/6-311G**) yields a value of 1.16 eV [16]. G2 theory, a SCF-based sequence of Møller-Plesset perturbation calculations using basis sets with up to one f function for sulfur, augmented by partly semiempirical corrections for the incompleteness of the one- and many-particle spaces, almost matches the experimental value (1.670 ± 0.015 eV) with a prediction of 1.66 eV [48]. On the basis of the calibration studies performed in the present study it seems that the surprisingly good G2 results may partly be due to error cancellation. Finally, we would like to mention that with a mixed density-functional–Hartree-Fock approach, the electron affinity of S_2 has been calculated as 1.51 eV [48].

We have included the theoretical vertical electron affinities (VEAs) and vertical detachment energies (VDEs) in Table VI. These quantities refer to the energies of electron attachment to S_2 at its equilibrium internuclear distance (VEA) and electron detachment from S_2^- at the minimum of its ground-state potential-energy curve (VDE), respectively (see Fig. 2). They may be of interest for special types of electron transfer experiments.

TABLE VI. Adiabatic (AEA) and vertical (VEA) electron affinities for S_2 and vertical detachment energies (VDE) for S_2^- (in eV). The zero-point vibrational energy contribution is not included and amounts to -0.01 eV. Values in parentheses have been obtained with the $7s6p4d3f$ ANO contraction.

Method	AEA	VEA	VDE
SCF	0.99	0.73	1.25
CAS-SCF	0.66 (0.65)	0.44	0.73
MRCI	1.29 (1.25)	1.14	1.43
MRCI+Q	1.48 (1.42)	1.32	1.62
CCSD	1.65	1.52	1.84
CCSD(T)	1.65	1.46	1.78
Expt.	1.670 ± 0.015		

E. Binding energies of triatomic sulfur clusters

In a recent investigation [9(b)], we have investigated the neutral and anionic S_3 clusters in a variety of properties. From this starting point the present study of S_2 and S_2^- thus enables one to calculate the binding energies of the neutral and anionic S_3 clusters, both of which, as we have demonstrated, exhibit a C_{2v} molecular geometry in their electronic ground states. Since we have not computed the bond separation pathways on the potential-energy surfaces corresponding to the reactions $S_3 \rightarrow S_2 + S$ and $S_3^- \rightarrow S_2 + S^-$, the size-extensive coupled-cluster method has been employed to compute the binding energies from the separated fragments. The results of these calculations are summarized in Table VII. Zero-point vibrational energies (ZPEs) have not explicitly been includ-

TABLE VII. Binding energies of the neutral and anionic trisulfur clusters (in kcal/mol) using MRCI+Q optimized geometries for S_x and S_x^- [9(b)].

Cluster	SCF	CCSD	CCSD(T)	Expt. [49]
$S_3 \rightarrow S_3 + S$	10.9	51.0	59.4	65.6
$S_3^- \rightarrow S_2 + S^-$	20.2	64.0	67.8	66.3

ed, but it can be estimated that the ZPEs of S_3 and S_3^- are approximately 0.1 eV [9(b)] while those of S_2 and S_2^- have been calculated as 0.05 and 0.04 eV in the present study (see Table V). The resulting ZPE correction of 0.05 eV (1 kcal/mol) for the binding energy of the S_3 and S_3^- cluster is thus in the overall uncertaincy of the theoretical predictions.

The experimental binding energies for the neutral S_3 and the anionic S_3^- clusters amount to 65.6 kcal/mol ($S_3 \rightarrow S_2 + S$) and 66.3 kcal/mol ($S_3^- \rightarrow S_2 + S^-$), respectively [49]. As expected, the binding energies are severely underestimated at the single-configuration Hartree-Fock SCF level (for $S_3 \rightarrow S_2 + S$, + 10.9 kcal/mol and for $S_3^- \rightarrow S_2 + S^-$, +20.2 kcal/mol). The CCSD calculations recover a large part of the correlation corrections and reduce the errors with respect to experiment to 14.6 kcal/mol (S_3) and 2.3 kcal/mol (S_3^-), respectively. Inclusion of the perturbative treatment of the triple contributions CCSD(T) yields binding energies of 59.1 kcal (S_3) and 67.8 kcal/mol (S_3^-).

It appears that the theoretical binding energies for the anionic S_3^- cluster show overall better agreement with the experimental results compared to the neutral S_3 case at all levels of theory considered here. The better agreement between experimental and theoretical binding energies for the neutral S_3 cluster is once more due to the more pronounced multireference character of one species in the bond separation processes: As shown in our previous study [9(b)], at least two valence configurations are necessary to describe the ground state of S_3, whereas S_3^- can be regarded as a more simple single-reference problem. Since the weights of the Hartree-Fock functions in CAS-SCF or MRCI expansions are smaller for the triatomic than for the diatomic species, it follows that the underestimation of the binding energies at the Hartree-Fock level is due to an insufficient description of the triatomic clusters with respect to its constituents. This effect is more pronounced in the neutral than in the anionic case. The correlated calculations, at least at the CCSD level, are still biased due to their Hartree-Fock reference, although the overall agreement with experiment is much better. Furthermore, the triple contributions enhance the binding energy by 8 kcal/mol for S_3 but only 4 kcal/mol for S_3^-, which shows that at the CCSD level, the deficiencies in the description of S_3 are more pronounced compared to S_3^-. Earlier calculations have been reported for the neutral S_3 cluster [50]. Here the QCISD(T)-6-31G* method gave a binding energy of 38.9 kcal/mol, which is considerably lower than the result reported here, due to the relatively low level in both the employed basis set and correlation treatment.

F. Low-lying electronic states of S_2^-

The spectrum of the electronic states of S_2^- considered in this study is displayed in Fig. 3. Corresponding total MRCI+Q energies and spectroscopic constants are listed in Tables IV and V. The excited states will be discussed in their energetic ordering relative to the $^2\Pi_g$ ground state.

1. $^4\Sigma_u^-$ state

The lowest-lying excited state of S_2^- arises upon excitation of an electron from the antibonding π_g 3*p* orbital into the empty antibonding σ_u 3*p* orbital and a parallel coupling of the unpaired electrons (see Tables I and III). An adiabatic excitation energy of 2.13 eV or 17 185 cm^{-1} is required for this spin-forbidden process. Although there exit only four symmetry-adapted reference configurations for the $^4\Sigma_u^-$ state (see Table I), the electronic situation is far from the simple one-electron picture described above with a weight of only 78.7% for the Hartree-Fock configuration in the total MRCI expansion. The equilibrium internuclear separation in this state (4.512 bohrs) is somewhat longer than in the ground state (3.815 bohrs) and a weakening of the S—S bond is also apparent from the lower vibrational frequency (270 cm^{-1} compared to 582 cm^{-1} in the ground state).

2. $^2\Pi_u$ (I) state

In the orbital picture, this state is generated from the ground state by promoting an electron from the bonding π_u 3*p* orbital to the hole in the antibonding π_g 3*p* orbital. Consequently, both the equilibrium internuclear distance (4.469 bohrs) and the vibrational frequency (340 cm^{-1}) are lower compared to the ground state. The adiabatic excitation energy from the ground state amounts to 2.40 eV (19 353 cm^{-1}). This lowest excited doublet state has 77.3% (see Table III) weight for its Hartree-Fock configuration in the MRCI expansion and is thus of similar multiconfigurational character as the $^4\Sigma_u^-$ state.

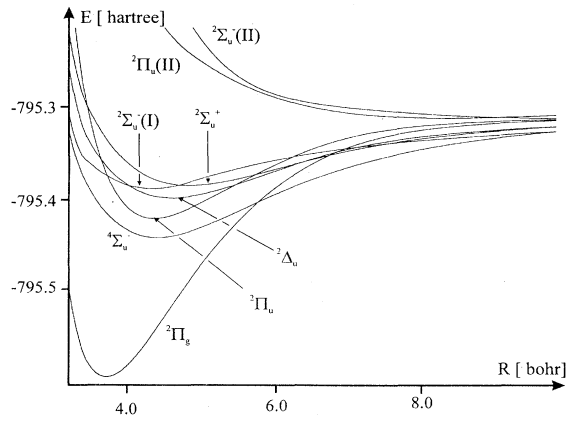

FIG. 3. Spectrum of the low-lying electronic states of S_2^- considered in this study.

3. $^2\Delta_u$ state

The $^2\Delta_u$ state is the first out of a series of three close-lying states for which an intuitive molecular-orbital description is no longer valid. As is evident from Table III, no fewer than six CSFs have weights greater than 5% in the MRCI expansion. Furthermore, the weight of the most important configuration, which has three doublet-coupled unpaired electrons in the π_g 3p and σ_u 3p orbitals, amounts to only 53.6%. A second configuration with a MRCI weight of 17.8% shows the same occupation pattern with a different spin coupling (see Table III). The adiabatic excitation energy from the ground state amounts to 2.71 eV (21 854 cm^{-1}). The equilibrium internuclear distance (4.720 bohrs) is larger and the vibrational frequency (236 cm^{-1}) smaller as compared to the ground state.

4. $^2\Sigma_u^-(I)$ state

The two important CSFs of this state are identical to the $^2\Delta_u$ state, with the modification that their absolute weights (19.9% and 59.3%) are interchanged and the coupling in the MRCI expansion is with a negative sign, rather than with a positive, as in the $^2\Delta_u$ state (see Table III). Consequently, the spectroscopic constants (R_e=4.444 bohrs and ω_e=224 cm^{-1}) are very similar to the $^2\Delta_u$ state and the resulting potential-energy curves exhibit a similar shape with a crossing near R=4 bohrs (see Fig. 3).

5. $^2\Sigma_u^+$ state

This state has the highest degree of multireference character among all states considered here. Two CSFs with weights of 32.0% show the antibonding σ_u 3p orbital singly occupied and two paired electrons in one of the antibonding π_g 3p orbitals and are coupled by a positive sign in the MRCI expansion. Counterparts with the π_u 3p instead of the π_g 3p orbitals doubly occupied have weights of 10.6% each. The equilibrium internuclear distance (4.940 bohrs) is the largest and the vibrational frequency (205 cm^{-1}) the lowest among all states of S_2^- considered in this study. Energetically, the $^2\Sigma_u^+$ state is very close to the $^2\Sigma_u^-(I)$ and $^2\Delta_u$ states with an adiabatic excitation energy of 2.90 eV (23 371 cm^{-1}) from the $^2\Pi_g$ ground state.

6. $^2\Pi_u(II)$ state and $^2\Sigma_u^-(II)$ states

The second states of $^2\Pi_u$ and $^2\Sigma_u^-$ symmetry are repulsive along the whole internuclear range (see Fig. 2). Energetically, they lie relatively high at 7.41 and 9.54 eV above the ground state at the equilibrium internuclear distance of the latter.

The sequence of electronic states can qualitatively be compared to the situation in the O_2^- anion, which was theoretically investigated some time ago [7(a)]. As far as this earlier CAS-SCF and the present MRCI study can be compared, the situation in both anionic chalcogenide species is similar. The $^4\Sigma_u^-$ state is the lowest excited state above the $^2\Pi_g$ ground state in both cases. Furthermore, the $^2\Pi_u$(I) state has the smallest internuclear equilibrium distance among all excited states while the $^2\Pi_u$(II) and $^2\Sigma_u^-$(II) states are purely repulsive. The O_2^- study places the $^2\Sigma_u^+$, $^2\Sigma_u^-$(I), and $^2\Delta_u$ states below the $^2\Pi_u$(I) state. However, this treatment included only nondynamic correlation at the CAS-SCF level and the relative ordering of states may be quite different if an extensive CI treatment, as presented here for S_2^-, is included. In any case, also at the CAS-SCF level, the lowest excited doublet state of S_2^- is the $^2\Pi_u$(I) state.

The transition dipole moments between the ground state of S_2^- and all excited doublet states of ungerade symmetry are given in Table VIII. In absorption or luminescence experiments, the strongest band should occur for a transition between the $^2\Pi_g$ ground state and the excited state $^2\Pi_u$(I), between which the z component of the transition dipole matrix amounts to 1.0249 a.u. The vertical transition corresponding to this band is expected at 3.12 eV (25 172 cm^{-1} MRCI+Q energy difference), in good agreement with the maximum of the experimental absorption band at 25 600 cm^{-1} [1(b)]. For the 0-0 transition between the lowest vibronic levels of these two states we compute a value of 19 232 cm^{-1}, near the values reported for S_2^--doped alkaline iodides [3(c)] (for NaI, 19 087 cm^{-1}; for KI, 19 452 cm^{-1}; for RbI, 19 618 cm^{-1}), but about 1000 cm^{-1} lower as compared to the results for S_2^- in alkaline bromide and chloride ma-

TABLE VIII. Transition dipole moments between the ground state and excited states of S_2^- at R=3.815 bohrs (in a.u.).

Transition	Transition dipole moment[a] (component)	Transition energy[b] (eV)
$^2\Pi_g \rightarrow {}^2\Pi_u$	1.0249 (z)	3.31 (3.12)
$^2\Pi_g \rightarrow {}^2\Delta_u$	0.1898 (x,y)[c]	3.58 (3.22)
$^2\Pi_g \rightarrow {}^2\Sigma_u^+$	0.1505 (x,y)	3.99 (3.63)
$^2\Pi_g \rightarrow {}^2\Sigma_u^-$(I)	0.4597 (x,y)	3.50 (3.07)
$^2\Pi_g \rightarrow {}^2\Pi_u$(II)	0.2605 (z)	9.01 (7.41)
$^2\Pi_g \rightarrow {}^2\Sigma_u^-$(II)	0.0289 (x,y)	10.5 (9.54)

[a]Based on CAS-SCF wave functions: see Sec. II.
[b]CAS-SCF energies. MRCI transition energies at R=3.80 bohrs are given in parentheses.
[c] $^2\Delta_u$ as ^2A_u; the matrix element amounts to 0.1417 if the $^2\Delta$ state is calculated as $^2B_{1u}$.

TABLE IX. Spin-orbit coupling matrix elements (one-electron contributions) between the lowest quartet state ($^4\Sigma_u^-$) and various doublet states of S_2^- at $R = 3.815$ bohrs based on CAS-SCF wave functions; see Sec. II.

	Matrix element (cm^{-1}) (component)[a]	Transition energy[b] (eV)
$\langle {}^2\Pi_g \vert H_{s.o.} \vert {}^4\Sigma_u^- \rangle$	0	3.09
$\langle {}^2\Pi_u(I) \vert H_{s.o.} \vert {}^4\Sigma_u^- \rangle$	74 ($\langle \frac{1}{2} \vert H_{s.o.} \vert \frac{3}{2} \rangle$); 43 ($\langle \frac{1}{2} \vert H_{s.o.} \vert -\frac{1}{2} \rangle$)	0.23
$\langle {}^2\Delta_u \vert H_{s.o.} \vert {}^4\Sigma_u^- \rangle$	0	0.94
$\langle {}^2\Sigma_u^-(I) \vert H_{s.o.} \vert {}^4\Sigma_u^- \rangle$	0	1.24
$\langle {}^2\Sigma_u^+ \vert H_{s.o.} \vert {}^4\Sigma_u^- \rangle$	370 ($\langle \frac{1}{2} \vert H_{s.o.} \vert \frac{1}{2} \rangle$)	1.21

[a]The notation $\langle \Sigma_1 \vert H_{s.o.} \vert \Sigma_2 \rangle$ indicates that the nonvanishing value corresponds to the matrix element between a component of the $^4\Sigma_u^-$ state with $\Sigma = \Sigma_2$ and a component of a doublet state with $\Sigma = \Sigma_1$, where Σ denotes the spin projection on the internuclear axis.
[b]CAS-SCF energies.

trices (e.g., for KCl, 20 468 cm^{-1}) [3(c)]. The spin-orbit splitting of the $^2\Pi_g$ ground state is computed as 416 cm^{-1} (one-electron contributions, see Sec. II), which is the energy difference between the $\Omega = \frac{1}{2}$ and $\frac{3}{2}$ components, compared to experimental values of 440 [27], 420 [3(d),4(c)] and 410 cm^{-1} [5(e)]. For the excited $^2\Pi_u(I)$ state, the computed splitting amounts to 370 cm^{-1}, which places the spin-orbit correction to the 0-0 transition at approximately 50 cm^{-1}.

Thus we attribute the large difference between the calculated energy for the 0-0 transition of the free S_2^- ion and the experimental result for S_2^- in alkali bromide and chloride matrices to crystal-field effects that are not included in the quantum-chemical calculations. Moreover, the good agreement with the alkaline iodide data shows that these particular host matrices have relatively little influence on the spectroscopic properties of "guest" molecules, which we attribute to the fact that the iodide crystals are less ionic as compared to the lighter bromides and chlorides, resulting in smaller electrostatic fields and compressive crystal field effects. However, these examples show that the comparison of theoretical results for isolated molecules with results from matrix experiments is by no means straightforward and has to be carried out with caution [3(c)].

The transition intensities between other excited doublet states and the $^2\Pi_g$ ground state are much smaller: As the next intense band, we predict the vertical $^2\Pi_g \rightarrow {}^2\Sigma_g^-$ transition at 3.07 eV (24 769 cm^{-1} for the MRCI+Q), at about 25% of the intensity of the $^2\Pi_g \rightarrow {}^2\Pi_u(I)$ band (see Table VIII). Unfortunately, this transition is obscured in the experimental spectra by the more intensive $^2\Pi_g \rightarrow {}^2\Pi_u(I)$ process. Lower intensities are predicted for the $^2\Pi_g \rightarrow {}^2\Delta_u$ and $^2\Pi_g \rightarrow {}^2\Sigma_u^+$ transitions (transition matrix elements of 0.1898 and 0.1505 a.u., respectively) with vertical excitation energies of 3.22 eV (25 979 cm^{-1}) and 3.63 eV (29 287 cm^{-1}). Only the latter band, although relatively weak, may be expected to be seen separated from the intense $^2\Pi_g \rightarrow {}^2\Pi_u(I)$ band in a region around 340 nm in an electronic spectrum of S_2^-.

The matrix elements of the spin-orbit operator between bound states of different multiplicity are given in Table IX. Although they do not directly correspond to observables, these values can give a rough estimate of the probability of a transition between one of the doublet states and the low-lying $^4\Sigma_u^-$ state in S_2^- [51,52(b)]. The spin-orbit matrix elements between the $^2\Pi_g$ ground state as well as the excited $^2\Sigma_u^-(I)$ and $^2\Delta_u$ states with the $^4\Sigma_u^-$ state vanish by symmetry [52] while the $^2\Pi_u(I)$ and $^2\Sigma_u^+$ states have nonzero coupling elements to the $^4\Sigma_u^-$ state via the spin-orbit operator. Since a nonzero matrix element requires the same value for Ω ($\Omega = \Lambda + \Sigma$, where Λ and Σ denote the projections of the total orbital angular momentum and spin on the internuclear axis) in both states the $\Sigma = \pm\frac{1}{2}$ components of the $^2\Sigma_u^+(\Lambda = 0)$ state are coupled to the $\Sigma = \pm\frac{1}{2}$ components of the $^4\Sigma_u^-(\Lambda = 0)$ state (see Table IX). The same argument requires that the $\Sigma = +\frac{1}{2}$ ($-\frac{1}{2}$) component of the $^2\Pi_u(I)$ ($\Lambda = 1$) state is coupled to both the $\Sigma = +\frac{3}{2}$ ($+\frac{1}{2}$) and the $\Sigma = -\frac{1}{2}$ ($-\frac{3}{2}$) components of the $^4\Sigma_u^-(\Lambda = 0)$ state. The larger coupling is recognized for the $^2\Sigma_u^+$-$^4\Sigma_u^-$ (370 cm^{-1}) case, for which the spin-orbit coupling matrix element is five times larger as compared to the $^2\Pi_u$-$^4\Sigma_u^-$ interaction (74 and 43 cm^{-1}). The results may be interpreted in the sense that the lifetime of the $^4\Sigma_u^-$ state, once generated from one of the electronically excited doublet states, may be long enough to allow for a spectroscopic detection, since the spin-orbit coupling to the only state that lies lower in energy, the $^2\Pi_g$ ground state, is zero by symmetry. In particular, it seems that direct transitions to the low-lying quartet state should proceed favorably from the excited $^2\Sigma_u^+$ state via a mechanism involving spin-orbit coupling. However, we stress that the actual probability of a doublet-quartet transition will also depend on several additional factors.

ACKNOWLEDGMENTS

The authors would like to acknowledge helpful discussions with J. Natterer. This work was supported by the Fonds der Chemischen Industrie (C.H.) and the Gesellschaft der Freunde der Technischen Universität Berlin. We thank the Konrad-Zuse Zentrum Berlin for a generous allotment of computer time.

[1] Data for the diatomic anions are found in (a) J. Rolfe, R. F. Lipsett, and W. J. King, Phys. Rev. **123**, 447 (1961); (b) G.-G. Lindner, Ph.D. thesis (Shaker, Aachen, 1994). Data for the triatomic anions are found in (c) L. Andrews, J. Am. Chem. Soc. **95**, 4487 (1973); (d) H. Bill and W. Von der Osern, Phys. Status Solidi B **75**, 613 (1978); (e) W. E. Thompson and M. E. Jacox, J. Chem. Phys. **91**, 3826 (1989); (f) G. Steffen, W. Hesse, M. Jansen, and D. Reinen, Inorg. Chem. **30**, 1923 (1991); see also (b).

[2] Data for the diatomic anions are found in (a) K. Nakamoto, *Infrared and Raman Spectra of Inorganic and Coordination Compounds,* 3rd ed. (Wiley, New York, 1977); (b) Ref. [1(b)]. Data for the triatomic anions are found in (c) R. J. H. Clark, T. J. Dines, and M. Curmoo, Inorg. Chem. **22**, 2766 (1983).

[3] Data for the diatomic anions are found in (a) J. Rolfe, J. Chem. Phys. **49**, 4193 (1968); (b) W. Holzer, W. F. Murphy, and H. J. Bernstein, J. Mol. Spectosc. **32**, 13 (1969); (c) M. Ikezawa and J. Rolfe, J. Chem. Phys. **58**, 2024 (1973); (d) G. J. Vella and J. Rolfe, *ibid.* **61**, 41 (1974); (e) V. E. Bondybey and J. H. English, *ibid.* **72**, 6479 (1980); (f) J. S. Cook, J. S. Dryden, and J. Ferguson, J. Lumin. **36**, 1 (1986); (g) H. Fabian and F. Fischer, *ibid.* **43**, 103 (1989); (h) H. Murata, T. Kishigami, and R. Kato, J. Phys. Soc. Jpn. **59**, 506 (1990); (i) Ref. 1(b).

[4] Data for the diatomic anions are found in (a) R. F. Barrow, B. B. Chandler, and C. B. Meyer, Philos. Trans. R. Soc. (London) Ser. A **260**, 395 (1966); (b) J. R. Morton, J. Chem. Phys. **71**, 89 (1967); (c) L. E. Vannotti and J. R. Morton, Phys. Rev. **161**, 282 (1967); (d) P. W. Atkins and M. C. R. Simons, *The Structure of Inorganic Radicals* (Elsevier, Amsterdam, 1967); (e) J. A. Rabo, *Zeolithe Chemistry and Catalysis,* ACS Monograph No. 171 (American Chemical Society, Washington, DC, 1976). Data for the triatomic anions are found in (e) L. E. Vanotti, and J. R. Morton, Phys. Rev. **161**, 282 (1968); (f) J. M. de Siebenthal and H. Bill, Phys. Status Solidi B **91**, 479 (1979); (g) N. M. Atherton, J. R. Morton, K. F. Preston, and S. J. Strach, J. Chem. Phys. **74**, 5521 (1981).

[5] For data on O_2^- (a) R. J. Celotta, R. A. Bennett, J. L. Hall, M. W. Siegel, and J. Levine, Phys. Rev. A **6**, 631 (1972); (b) M. J. Travers, D. C. Cowles, and G. B. Ellison, Chem. Phys. Lett. **164**, 449 (1989). For data on O_3^- see (c) S. E. Novick, P. C. Engelking, P. L. Jones, J. H. Futrell, and W. C. Lineberger, J. Chem. Phys. **70**, 2652 (1979). For a recent combined experimental-theoretical study of the low-lying states of O_3^-, see (d) D. W. Arnold, C. Xu, E. H. Kim, and D. M. Neumark, J. Chem. Phys. **101**, 912 (1994); for S_2^- see (e) S. Moran and G. B. Ellison, J. Phys. Chem. **92**, 1794 (1988); for S_3^- see (f) M. R. Nimlos and G. B. Ellison, *ibid.* **90**, 2574 (1986); for Se_2^-, Se_3^-, Te_2^-, and Te_3^- see (f) J. T. Snodgrass, J. V. Coe, K. M. McHugh, C. B. Freidhoff, and K. H. Bowen, *ibid.* **93**, 1249 (1989).

[6] J. G. Dillard and J. L. Franklin, J. Chem. Phys. **48**, 2349 (1968); T. Schindler, C. Berg, G. Niedner-Schatteburg, and V. E. Bondybey, Ber. Bunsenges. Phys. Chem. **96**, 1114 (1992).

[7] (a) M. Krauss, D. Neumann, A. C. Wahl, G. Das, and W. Zemke, Phys. Rev. A **7**, 69 (1973). (b) Further studies on parts of the electronic spectrum of O_2^- are found in G. Das, A. C. Wahl, W. T. Zemke, and W. C. Stwalley, J. Chem. Phys. **68**, 4252 (1978); G. Das, W. T. Zemke, and W. C. Stwalley, *ibid.* **72**, 2327 (1980); K. J. Borve and P. E. M. Siegbahn, Theor. Chim. Acta **77**, 409 (1990).

[8] (a) W. Koch, G. Frenking, G. Steffen, D. Reinen, M. Jansen, and W. Assenmacher, J. Chem. Phys. **99**, 1271 (1993); (b) Ref. 5(c).

[9] (a) W. von Niessen and P. Tomasello, J. Chem. Phys. **87**, 5333 (1987); (b) W. Koch, J. Natterer, and C. Heinemann, *ibid.* **102**, 6159 (1995).

[10] Representative case studies for triatomic molecules of the sixth main group are found in H. Basch, Chem. Phys. Lett. **157**, 129 (1989); W. von Niessen, L. S. Cederbaum, and F. Tarantelli, J. Chem. Phys. **91**, 3582 (1989); R. González-Luque, M. Merchán, P. Borowski, and B. O. Roos, Theor. Chim. Acta **86**, 467 (1993); V. G. Zakrewski and W. van Niessen, *ibid.* **88**, 75 (1994); see also Ref. [8].

[11] T. Noro, M. Yoshimine, M. Sekiya, and F. Sasaki, Phys. Rev. Lett. **66**, 1157 (1991); R. A. Kendall, T. H. Dunning, and R. J. Harrison, J. Chem. Phys. **96**, 6796 (1992).

[12] R. J. Celotta, R. A. Bennett, and J. L. Hall, J. Chem. Phys. **60**, 1740 (1974). This earlier PE study of S_2^- gave an electron affinity for S_2 of 1.663 ± 0.004 eV and a vibrational frequency of 524 ± 121 cm^{-1} for the electronic ground state of S_2^-.

[13] C. E. Moore, *Atomic Energy Levels,* Natl. Bur. Stand. Ref. Data Ser., Natl. Bur. Stand. (U.S.) Circ. No. 35 (U.S. GPO, Washington, DC, 1971), Vol. 1.

[14] F. A. Cotton, J. B. Harmon, and R. M. Hedges, J. Am. Chem. Soc. **98**, 1417 (1976).

[15] F. Ramondo, N. Sanna, and L. Bencivenni, J. Mol. Struc. (THEOCHEM) **258**, 361 (1992).

[16] L. A. Curtiss, K. Raghavachari, G. W. Trucks, and J. A. Pople, J. Chem. Phys. **94**, 7221 (1991).

[17] C. Heinemann, W. Koch, G.-G. Lindner, and D. Reinen (unpublished).

[18] For a detailed description of the method, see P. E. M. Siegbahn, in *Lecture Notes in Quantum Chemistry,* edited by B. O. Roos, Lecture Notes in Chemistry Vol. 58 (Springer, Berlin, 1992), p. 255.

[19] For a recent discussion of this topic, see W. Duch and G. H. F. Diercksen, J. Chem. Phys. **101**, 3018 (1994).

[20] B. O. Roos, Adv. Chem. Phys. **69**, 399 (1987); in *Lecture Notes in Quantum Chemistry* (Ref. [18]), p. 177.

[21] Correlating the 2*s* and 2*p* electrons requires special functions in the one-particle basis sets that are not included in the ANO basis sets employed here. See, e.g., P. R. Taylor, in *Lecture Notes in Quantum Chemistry* (Ref. [18]), p. 325. For a recent study of 1*s* correlation effects in N_2, see C. W. Bauschlicher and H. Partridge, J. Chem. Phys. **100**, 4329 (1994).

[22] For details on MOLCAS-2 see the respective user's manual: K. Anderson, M. R. A. Blomberg, M. P. Fülscher, V. Kellö, R. Lindh, P.-A. Malmquist, J. Noga, J. Olsen, B. O. Roos, A. J. Sadlej, P. E. M. Siegbahn, M. Urban, and P.-O. Widmark, University of Lund, 1991.

[23] E. R. Davidson, in *The World of Quantum Chemistry,* edited by R. Daudel and B. Pullmann (Reidel, Dordrecht, 1974); S. R. Langhoff and E. R. Davidson, Int. J. Quantum Chem. **8**, 61 (1974); E. R. Davidson and D. W. Silver, Chem. Phys. Lett. **52**, 403 (1977).

[24] P. A. Malmquist and B. O. Roos, Chem. Phys. Lett. **155**, 189 (1989).

[25] For excellent reviews, see R. J. Bartlett, J. Phys. Chem. **93**, 1697 (1989); R. J. Bartlett and J. F. Stanton, in *Reviews in Computational Chemistry,* edited by K. B. Lipkowitz (VCH, New York, 1994), Vol. 5.

[26] T. E. H. Walker and W. G. Richards, J. Chem. Phys. **52**,

1311 (1970).
[27] S. Koseki, M. W. Schmidt, and M. S. Gordon, J. Phys. Chem. **96**, 10 768 (1992).
[28] (a) J. Almlöf and P. R. Taylor, J. Chem. Phys. **86**, 4070 (1986); (b) P.-O. Widmark, B. J. Perrson, and B. O. Roos, Theor. Chim. Acta **79**, 419 (1991).
[29] A. D. McLean and G. S. Chandler, J. Chem. Phys. **72**, 5639 (1980).
[30] ACES−2, version 1.0, University of Florida, Gainesville, FL, 1993; J. F. Stanton, J. Gauss, J. D. Watts, W. J. Lauderdale, and R. J. Bartlett, Int. J. Quantum Chem. Symp. **26**, 879 (1992).
[31] MOLPRO is a package of *ab initio* programs written by H.-J. Werner and P. J. Knowles with contributions from J. Almlöf, R. D. Amos, M. J. O. Deegan, S. T. Elbert, C. Hampel, W. Meyer, K. Peterson, R. Pitzer, A. J. Stone, and P. R. Taylor. The open-shell coupled-cluster part of MOLPRO is described in P. J. Knowles, C. Hampel, and H.-J. Werner, J. Chem. Phys. **99**, 5219 (1993).
[32] M. W. Schmidt, K. K. Baldridge, J. A. Boatz, J. H. Jensen, S. Koseki, M. S. Gordon, K. A. Nguyen, T. L. Windus, and S. T. Elbert, Quantum Chemistry Program Exchange Bull. **10**, 52 (1990).
[33] The exact experimental result is 2.077 120(1) eV, from H. Hotop and W. C. Lineberger, J. Phys. Chem. Ref. Data **14**, 731 (1985).
[34] D. E. Woon and T. H. Dunning, J. Chem. Phys. **98**, 1358 (1993).
[35] Adding one additional diffuse *s*-type (exponent 0.02) and one *p*-type (exponent 0.01) function to the ANO3 contraction increases the CCSD(T) electron affinity by only 0.001 eV.
[36] The VFCI calculations were performed with the determinant based code included in the MOLPRPO94 program: P. J. Knowles, N. C. Handy, Chem. Phys. Lett. **111**, 315 (1984); P. J. Knowles and N. C. Handy, Comput. Phys. Commun. **54**, 75 (1989).
[37] Total energies for S(^3P) are −397.646 55 (CISD), −397.657 13 (CISD-Q), −397.654 75 [CCSD(T)], and −397.656 13 (VFCI). The total energies for S^-(^2P) are −397.708 89 (CISD), −397.724 50 (CISD+Q), −397.724 62 [CCSD(T)], and −397.726 17 (VFCI).
[38] One-particle spaces of this size have been characterized as "balanced" when used in connection with the CCSD(T) method: J. R. Thomas, B. J. DeLeeuw, G. Vacek, T. D. Crawford, Y. Yamaguchi, and H. F. Schaefer, J. Chem. Phys. **99**, 403 (1993).
[39] These calculations were carried out using the finite field perturbation theory part of the MOLCAS−2 suite of programs: V. Kellö, A. J. Sadlej, J. Chem. Phys. **93**, 8122 (1990).
[40] For a discussion of core-valence and core-core correlation effects in beryllium and carbon atoms, see C. W. Bauschlicher, S. R. Langhoff, and P. R. Taylor, J. Chem. Phys. **88**, 2540 (1988).
[41] P. R. Taylor, Mol. Phys. **49**, 1297 (1983).
[42] G. Herzberg, *Molecular Spectra and Molecular Structure* (Krieger, Malabar, FL, 1989), Vol. 1.
[43] R. González-Luque, M. Merchán, M. P. Fülscher, and B. O. Roos, Chem. Phys. Lett. **204**, 323 (1993).
[44] A. Szabo and N. S. Ostlund, *Modern Quantum Chemistry*, 2nd ed. (McGraw-Hill, New York, 1989).
[45] S. F. Boys and F. Bernardi, Mol. Phys. **19**, 553 (1970).
[46] S. Wilson, Adv. Chem. Phys. **67**, 439 (1987). For a recent discussion of the definition of the BSSE, see E. R. Davidson and S. J. Chakravorty, Chem. Phys. Lett. **217**, 48 (1994).
[47] S. A. Kucharski and R. J. Bartlett, J. Chem. Phys. **95**, 8227 (1991); A. Balková and R. J. Bartlett, J. Chem. Phys. **102**, 7116 (1995).
[48] P. M. W. Gill, B. G. Johnson, J. A. Pople, and M. J. Frisch, Int. J. Quantum Chem. Quantum Chem. Symp. **26**, 319 (1992).
[49] NIST Negative Ion Energetics Database, Version 3.01, edited by J. E. Bartmess, Gaithersburg, MD, 1993.
[50] K. Raghavachari, C. McMichael Rohlfing, and J. S. Binkley, J. Chem. Phys. **93**, 5862 (1990).
[51] See the discussion in P. J. Bruna and S. D. Peyerimhoff, Adv. Chem. Phys. **67**, 1 (1987); S. R. Langhoff, J. Chem. Phys. **73**, 2379 (1980).
[52] (a) K. Kayama and J. C. Baird, J. Chem. Phys. **46**, 2604 (1967); (b) H. Levèbvre-Brion, R. W. Field, *Perturbations in the Spectra of Diatomic Molecules* (Academic, Orlando, 1986).